Journal of Catalysis **209,** 489–500 (2002)
doi:10.1006/jcat.2002.3653

Relation between Electronic Structure of α-Substituted Ketones and Their Reactivity in Racemic and Enantioselective Platinum-Catalyzed Hydrogenation

Angelo Vargas, Thomas Bürgi, Matthias von Arx, Reto Hess, and Alfons Baiker[1]

Laboratory of Technical Chemistry, Swiss Federal Institute of Technology, ETH Hönggerberg, CH-8093 Zurich, Switzerland

Received January 25, 2002; revised March 1, 2002; accepted April 17, 2002

The relation between the electronic structure of α-substituted ketones and their reactivity in the racemic and enantioselective platinum-catalyzed hydrogenation has been investigated using a combined theoretical and experimental approach. A correlation between the keto carbonyl orbital energy and the hydrogenation rate has been found, which rationalizes the effect of the substituent on the rate of hydrogenation. The uncovered relationship between the keto carbonyl orbital energy and the hydrogenation rate provides a rational explanation for the often observed rate acceleration that occurs when cinchona-modified platinum is used as a enantioselective hydrogenation catalyst. The previously suggested model for enantiodiscrimination based on the different stability of the diastereomeric complexes formed between the reactant and the cinchona modifier is discussed in the light of the new kinetic findings.

Key Words: **α-substituted ketones; racemic hydrogenation; enantioselective hydrogenation; molecular modeling; electronic structure; reactivity; platinum; acetophenone; trifluoroacetophenone.**

1. INTRODUCTION

The enantioselective hydrogenation of α-substituted ketones on cinchona-modified platinum belongs, together with the enantioselective hydrogenation of β-keto esters on tartaric acid-modified nickel, to the most studied reactions in the field of enantioselective heterogeneous catalysis (1). The present state of knowledge concerning the functioning of the cinchona-modified platinum system has been covered in recent reviews (2–6). Although considerable progress has been made toward understanding the catalytic system, several aspects need further clarification. A comprehensive model should explain the often observed rate acceleration that occurs upon platinum modification with cinchona alkaloids and also include a discussion of the kinetic aspects of the hydrogen addition in relation to the asymmetric induction. A one-to-one interaction model according to which the formation of a complex between the alkaloid and the substrate is the origin of the enantiodifferentiation has been proposed (3, 7, 8). This model identifies the critical interaction as a hydrogen bond formed between the adsorbed alkaloid and the adsorbed substrate. The energy difference between the diastereomeric complexes leading to the *R*- or *S*-product has been calculated at different levels of theory and for different modifier–reactant pairs (3, 6, 7, 9, 10), including synthetic modifiers (11). Comparison of the theoretical results with the experimental findings indicated that the stability of the different diastereomeric complexes on the metal surface is crucial for enantiodifferentiation. As a consequence such stability considerations were proposed as a valuable guide in the design of efficient enantiodifferentiating modifier–reactant pairs (6, 12). However, none of the proposed models includes further details regarding the hydrogen addition. All concepts used are of a thermodynamic nature and consider energy differences between states of equilibrium, while kinetic phenomena, which imply the modification of the transition state energy, are not explicitly included in the descriptions. One of the main assumptions of the model was in fact that the pro(*R*) and the pro(*S*) interaction complexes are hydrogenated at the same rate, as graphically exemplified in Scheme 1a, where both reaction pathways are shown to have the same activation barrier, although starting from energetically different states. A distinct exception to this postulate is the observation that in principle the less stable of the two diastereomeric complexes could have a higher hydrogenation rate (13), which would lead to favored formation of the enantiomer opposite the one predicted by the model (Scheme 1b). For completeness of the kinetic picture Scheme 1 shows also a third possible reaction diagram, corresponding to the case in which the more stable of the two diastereomeric complexes also has a smaller activation barrier, therefore leading to a higher hydrogenation rate. In this last case the thermodynamic effect (which results in a major presence of the more stable complex) acts in the same direction as the kinetic effect, so that the major diastereomeric complex also is the most reactive. Despite this complex kinetic picture, all cases studied with our previously

[1] To whom correspondence should be addressed. Fax: +41(1) 632 11 63. E-mail: baiker@tech.chem.ethz.ch.

0021-9517/02 $35.00

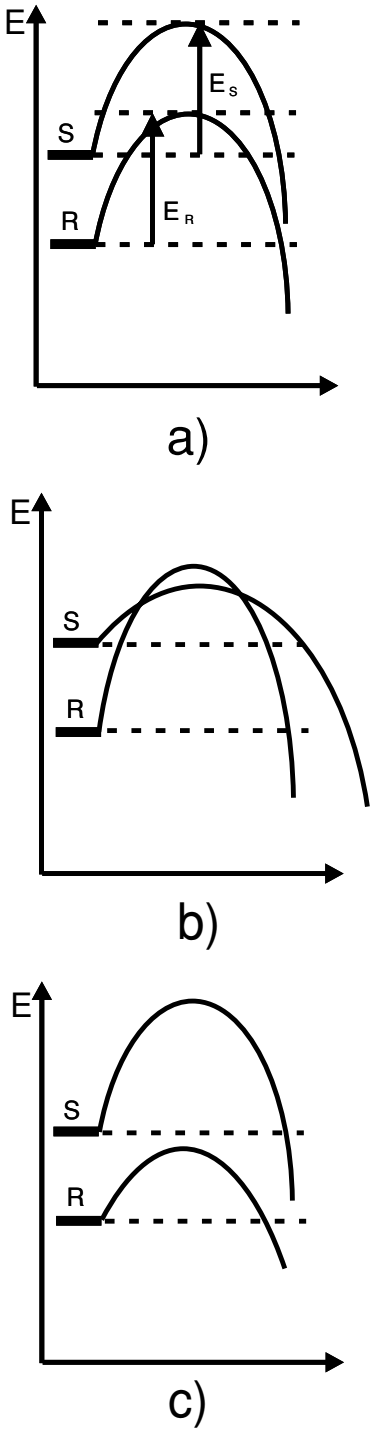

SCHEME 1. Thermodynamic (stability of diastereomeric complexes) and kinetic factors (activation energy of hydrogenation) affecting the sense of enantiodifferentiation: (a) $E_S = E_R$, (b) $E_S < E_R$, (c) $E_S > E_R$.

suggested model showed very good agreement between the model predictions and the direction of the enantiomeric induction, leading sometimes to an almost quantitative description of the experimentally achieved enantiomeric excess (ee). In order to gain a better understanding of the role played by the kinetic factors and possibly include them in the description, we have investigated in the present work the reaction rates for hydrogenation of a series of acetophenone and trifluoroacetophenone derivatives, in relation to their electronic structure. This series of aromatic ketones was chosen due to the possibility of tuning their reactivity via ring substitution. In a first step their reactivity toward racemic hydrogenation on an unmodified platinum catalyst was studied experimentally under standardized conditions and the kinetic results were correlated to selected orbital energies of the substrates. This analysis was also extended to acetophenone derivatives whose hydrogenation kinetics on palladium has been studied by Van Bekkum and co-workers (14). The result of this investigation converged to a proposed reaction mechanism, which accounts for the characteristic features (enantiodifferentiation, rate acceleration) observed in enantioselective hydrogenation. Hydrogen bonding is identified as critical for the kinetic as well as for the thermodynamic description of the reactivity. Thermodynamics and kinetics can be conceptually distinguished but are shown to be closely related for this system, because they depend on the same interaction.

2. METHODS AND EXPERIMENTAL

The electronic structure of the molecules in the study was analyzed aiming at identifying the bonding and antibonding orbitals of the keto carbonyl moiety and their relative energies. Orbital energies are given with respect to those of acetophenone that was taken as reference compound. All structures were optimized at the HF/6-31G* level of theory, using the Gaussian program package (15). Charges were computed using the Mulliken (16) and CHELP (17) schemes. Molden (18) was used as graphical tool. All catalytic tests were carried out according to the procedure described in detail in (19). As a measure for reactivity, the amount of substrate hydrogenated per unit time in experiments of 2-h duration was applied. All substrates were used as received (Fluka, Aldrich). For the racemic hydrogenation the following procedure was followed: a 5 wt% Pt/Al_2O_3 catalyst (Engelhardt 4759) was prereduced in flowing hydrogen for 90 min at 400°C. After cooling to room temperature under a flux of hydrogen, the catalyst was transferred to the reactor while protected by argon from exposure to atmosphere. Hydrogenations were carried out in a 100-ml stainless steel autoclave equipped with a 50-ml glass liner, PTFE cap, and stirrer. Under standard conditions 42 ± 2 mg of catalyst, 1.84 mmol of substrate, and 5 ml of toluene solvent were stirred magnetically (1000 rpm) at room temperature under a constant hydrogen pressure of 10 bar (20). For the enantioselective hydrogenations, which have been described in detail elsewhere (20), 6.8 μmol of cinchonidine was added to the reaction mixture

together with the substrate. Other conditions were the same as for the racemic reaction.

3. RESULTS

3.1. Racemic Hydrogenation

The apparent rate of catalytic hydrogenation of ketones principally depends on the energy barrier toward hydrogenation but also on the adsorption strength of the reactant in the region where the rate is non-zero order with respect to the reactant. Van Bekkum and co-workers showed that the reaction was zero order with respect to acetophenone and substituted acetophenones for their experimental conditions (14). In order to verify that also under our conditions the hydrogenation of acetophenones could be considered zero order, or at least approximately zero order, some experiments were performed where the concentration of the reactant was varied and the initial rate was determined from the hydrogen consumption curves. Trifluoroacetophenone was used as a test compound. Four different concentrations of the substrate were considered: 0.051, 0.087, 0.125, and 0.198 mol/L. For each experiment 48 mg of the catalyst was used under otherwise standard conditions. The results of the hydrogen consumption curves showed that the reaction is approximately zeroth order with respect to the reactant also under our experimental conditions.

In order to gain some information about the mechanism of activation of the carbonyl group toward hydrogen addition we searched for correlations between reactivity and electronic structure for a series of differently substituted acetophenones. From a molecular orbital point of view the carbonyl π and π* (bonding and antibonding) orbitals play an important role in the formation of the new bond with hydrogen, as exemplified in Scheme 2. In the latter the molecular orbital interactions between hydrogen and π keto carbonyl orbitals are shown for clarity in both classical ways: as an energy-level diagram and as symmetry-allowed interaction between orbitals. Three orbitals of the substituted acetophenone have been taken into consideration: the keto carbonyl antibonding π* orbital, always corresponding to the LUMO of the molecule, and two bonding keto carbonyl π orbitals with the highest energy. These orbitals are shown for acetophenone in Fig. 1. The keto carbonyl bonding orbital mixes with the π system of the aromatic ring and is split into two molecular orbitals. In the following we call bonding orbital **1** the orbital for which the mixing with the π system of the aromatic moiety is *not* in phase, and we call bonding orbital **2** the one for which the mixing is in phase. Depending on the substitution, the carbonyl π orbital coefficients of the two bonding orbitals changed. Most of the substituted acetophenones had greater carbonyl π orbital coefficients for bonding orbital **1**, as illustrated for acetophenone in Fig. 1. The opposite was found for the substituted trifluoroacetophenones. Figures 2–5 show plots of

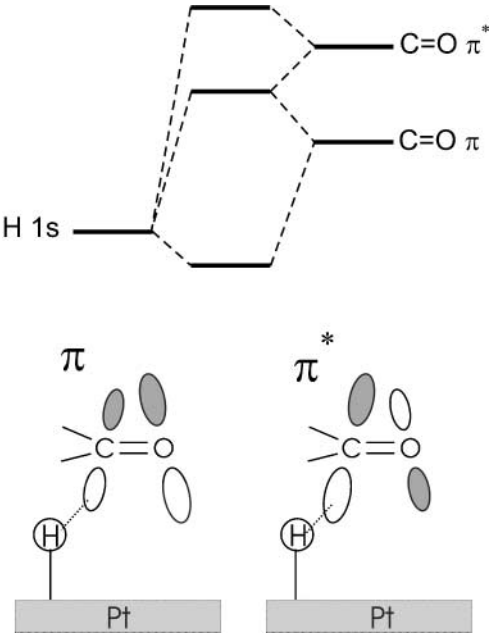

SCHEME 2. Molecular orbital interactions between the surface hydrogen and the bonding and antibonding π keto carbonyl orbitals of the ketone. Bottom: The dotted line indicates orbital interaction.

orbital energies and sums of orbital energies versus the rates of hydrogenation on the unmodified catalyst for a series of substituted acetophenones. Note that each plot corresponds to a different choice of orbitals. Reactivity depends on more than one orbital, and a linear combination of the orbital energies, with coefficients that are a function of their energy itself, would be the best choice. But these coefficients are unknown and therefore an empirical trial and error approach was used to estimate the specific orbital contribution. The plot in Fig. 2 refers to three orbitals: the keto carbonyl antibonding π* and the two keto carbonyl

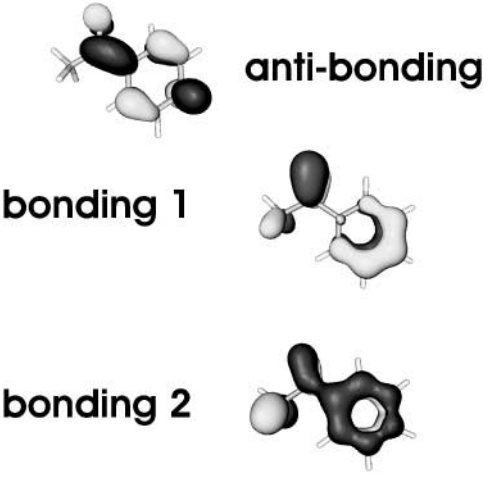

FIG. 1. Keto carbonyl antibonding and bonding orbitals (**1** and **2**) of acetophenone.

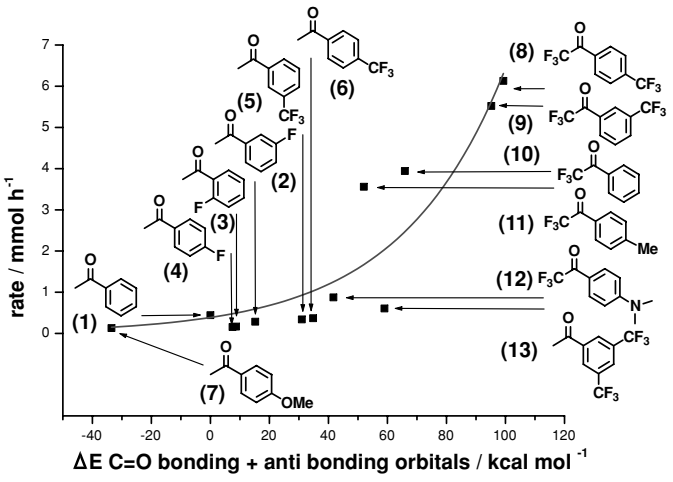

FIG. 2. Relationship between hydrogenation rate and energies of the keto carbonyl orbitals for a series of acetophenones. The orbital energies are relative to the corresponding acetophenone orbital energies. The plotted energy is the sum of the antibonding orbital and bonding orbitals **1** and **2**.

bonding π orbitals with the highest energies. From the energy of each of these orbitals of acetophenone, the energy of the corresponding one of the substituted acetophenone has been subtracted, and all energy differences have then been added. All positive numbers therefore correspond to orbitals that are more stable than the corresponding one in the acetophenone. A steep increase in reaction rate occurs at an orbital stabilization of 60–100 kcal/mol, although 3,5-di-trifluoromethyl acetophenone represents an exception. The plot presented in Fig. 3 refers to only one bonding orbital: the one that has the biggest orbital coefficient of the two bonding orbitals that are considered in Fig. 2. All derivatives of trifluoroacetophenone react faster than those

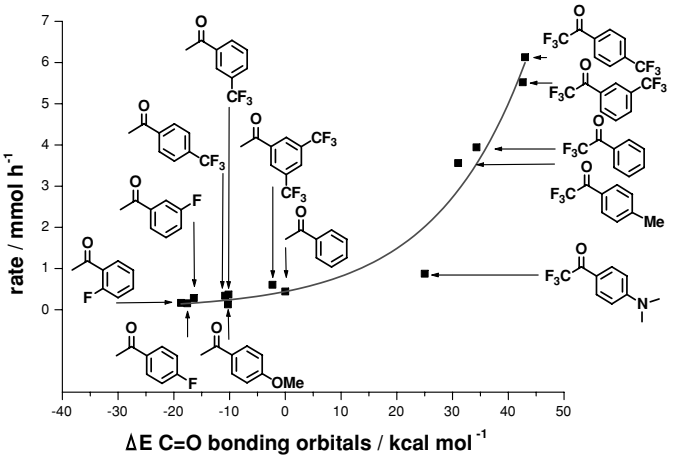

FIG. 3. Relationship between the hydrogenation rate and the energies of the bonding orbital alone for a series of acetophenones. The orbital energies are relative to the corresponding acetophenone orbital energies. Of the two keto carbonyl orbitals the one with the higher orbital coefficients was used.

of acetophenone, and they all have stabilized bonding keto carbonyl orbitals. Their reactivity can be further changed via ring substitution and the further stabilization of keto carbonyl bonding orbitals is followed by an increase in reaction rate. The first part of the curve reflects the behavior of acetophenone derivatives and shows a narrower variation of reactivity. In the range of 20 kcal/mol of orbital stabilization the rate varies between 0.1 and 0.6 mmol/h. The effect of the substituents is very different for the trifluoro acetophenones. In acetophenone a trifluoromethyl group in position 4 destabilizes the bonding keto carbonyl orbital by about 10 kcal/mol, and concomittantly the reaction rate decreases, while the same group at the same position causes a stabilization of ca. 15 kcal/mol in trifluoroacetophenone, and an increase in reaction rate. A similar effect can be noticed when position 3 instead of 4 is substituted. Note that in the case of the substitution in position 3 two conformations can be found according to the respective positions of the carbonyl moiety and the substituents in position 3, although rotational barriers to interconvert the two conformations are not high (below kT). Both the energies of the conformations and the respective orbital levels are very similar. It can be noticed that all substitutions tried on the acetophenone aromatic moiety raise the energy of the bonding C=O π orbital with respect to acetophenone, and all except the 3,5-di(trifluoromethyl) acetophenone also react slower, on the unmodified catalyst, than acetophenone. Concerning the effect of the substituents on the trifluoroacetophenones, a stabilization of the bonding keto carbonyl orbitals is obtained by trifluoromethyl substitution on the phenyl ring, while a destabilization is obtained by ring methylation and dimethylamino substitution in position 4. In particular the amino group in the para position strongly deactivates the compound toward hydrogen addition, restoring a level of reactivity similar to that of the ordinary acetophenones.

In Fig. 4 the antibonding orbitals energy stabilizations are plotted against the rate of hydrogenation. The exponential correlation is somehow less obvious. Substitution of CF_3 on the phenyl ring of acetophenone gives rise to a stabilization of the antibonding orbital, slightly more in the para than in the meta substitution, and only a slight increase in reaction rate is observed due to this change. All compounds except the O-methoxy acetophenone undergo keto carbonyl antibonding orbital stabilization. The trifluoroacetophenone derivatives also undergo a stabilization of the antibonding orbital, and the order of stabilization is the same as in the case of the bonding keto carbonyl orbitals.

Figure 5 shows the plot of the sum of the stabilizations of the bonding and antibonding orbitals against reaction rates. The contribution of the bonding orbitals has been taken from those that have the biggest orbital coefficients, as in Fig. 3. In this case again an exponential correlation is formed, however with slight changes in the sequence of the compounds on the curve with respect to Fig. 2. Figure 6 shows a logarithmic plot of the rates versus orbital energies

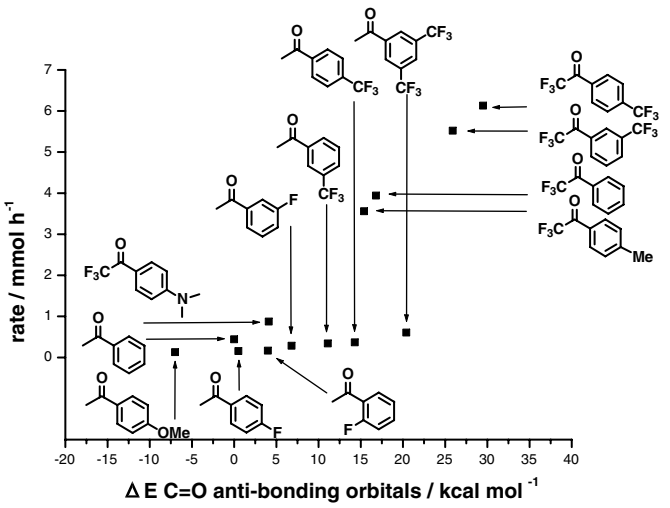

FIG. 4. Relationship between hydrogenation rate and energies of the antibonding orbitals for a series of acetophenones. The orbital energies are relative to the corresponding acetophenone orbital energies. The antibonding keto carbonyl orbital in all studied compounds corresponds to the LUMO orbital.

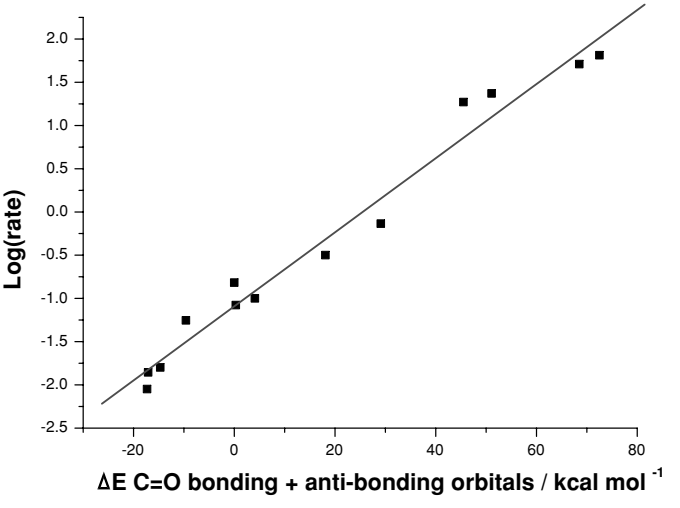

FIG. 6. Relationship between the logarithm of the hydrogenation rate and the sum of energies of the keto carbonyl orbitals (correlation coefficient, 0.99).

which resembles the linear free energy relationship of Hammett (21). We chose the carbonyl π orbitals energy as a correlating parameter because it allows us to investigate the effect of the enantiodifferentiating intermolecular interaction on this paramenter. Despite the energies of the carbonyl π orbitals the charge at the carbonyl carbon may be an important parameter reflecting reactivity. Figures 7 and 8 show plots of the carbonyl C atomic charge obtained by Mulliken analysis and by fitting atomic charges to the electrostatic potential derived from the calculated charge distribution, according to the CHELP method.

Mulliken charges behave quite rigidly to substitution, and substantial differences occur only between the acetophenone and trifluoroacetophenone derivatives groups. Hence, this scheme for charge calculation is not very sensitive to phenyl ring substitution. On the left hand sides of the graphic presentations (Figs. 7 and 8) are the molecules whose carbonyl carbon atoms are relatively more electron rich. The difference in charge between acetophenones and trifluoroacetophenones is slightly less than 0.2e and all acetophenone derivatives are more electron deficient than the respective trifluoroacetophenone derivatives. All the compounds that have high rates of hydrogenation belong to the relatively electron-rich ketones. The charge at the carbonyl C cannot be taken as a unique parameter for

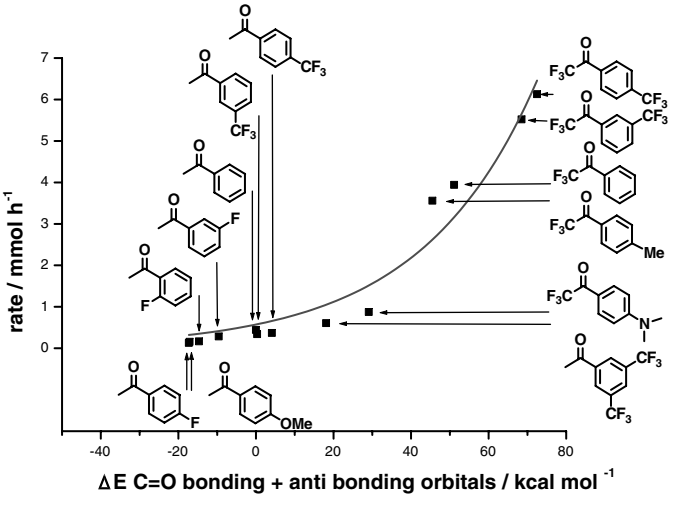

FIG. 5. Relationship between the hydrogenation rate and the sum of the energies of the keto carbonyl orbitals. The plotted energy ΔE is the sum of the antibonding orbital and the bonding orbital that has the higher orbital coefficient.

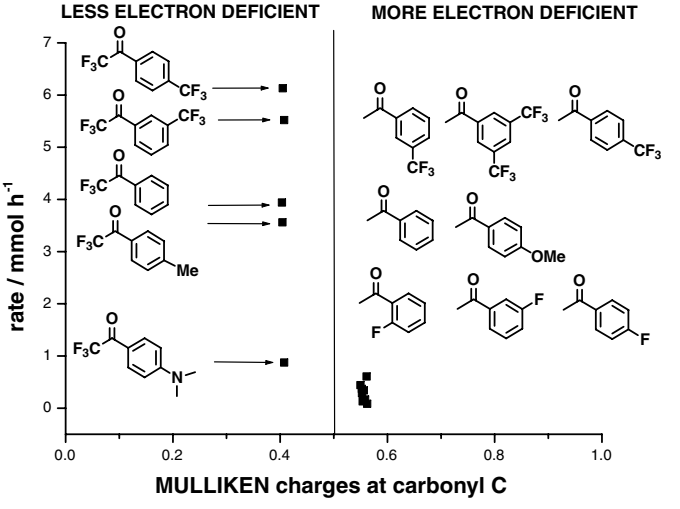

FIG. 7. Dependence of the hydrogenation rate and Mulliken charges of the carbonyl C for a series of acetophenones.

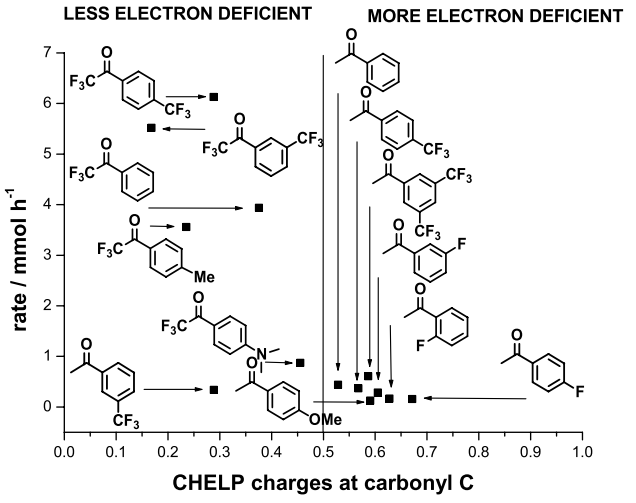

FIG. 8. Dependence of the hydrogenation rate and CHELP charges of the carbonyl C for a series of acetophenones.

reactivity. However, as a general trend an increase in reactivity is associated with an electronic charge increase at the carbonyl C.

Analyzing Fig. 8, where the CHELP charges are plotted against hydrogenation rate, we notice a greater sensitivity to the influence of the substituents. However, between the Mulliken and CHELP charges there is substantial accord. In fact both methods show that the fluorine atoms in the α-position cause electron enrichment of the carbonyl carbon. Furthermore both methods of analysis evidence a division of the molecules in two groups, α-fluorinated and non-α-fluorinated compounds. Within the series of the trifluoroacetophenones the most electron deficient is the 4-dimethylamino, which also has the smallest rate in the series. A complete correlation between charge at the carbonyl carbon and reactivity is nevertheless not apparent, as indicated for example by the fact that the most reactive compound, the 4-trifluoromethyl trifluoroacetophenone, has an intermediate position with respect to the charge. The position of the 3-trifluoromethyl acetophenone in the plot is rather odd. Its CHELP charge is 0.29e in the conformation considered in the graph, but 0.57e in the other possible conformation, which is more in line with what is found with the Mulliken scheme and more consistent with the other values. The two conformations of the 3-trifluoromethyl acetophenone have very similar orbital energies and the big charge difference has to be attributed to the sensitivity of the CHELP method on the conformation. The HOMO–LUMO gap has also been analyzed in correlation with the reaction rate for the series of acetophenones, but no correlation with their reactivity was found.

We applied the same strategy of correlating the carbonyl orbital energies to the reactivity toward hydrogenation for a series of acetophenones reported by Van Bekkum and co-workers (14). Note that the catalyst in this case was palladium and not platinum. Eleven compounds were chosen from those studied by Van Bekkum and co-workers, some of which correspond to the ones also used in our investigation. Figure 9 shows a plot of the stabilization of the keto carbonyl orbitals against the pseudo-zero-order kinetic constant. In the series couples of 3- and 4-substituted acetophenones are present for which a great variation in the kinetic constant had been observed, associated with the change in the position of the substituent. The amino- and O-methoxy-substituted acetophenones were more reactive for substitution in position 3, while the trifluoromethyl-, the carboxy-, and the acetyl-substituted acetophenones were more reactive when substituted in position 4. Table 1 gives the values calculated for the orbital stabilization of the bonding and antibonding keto carbonyl π orbitals, with the same criterion used for the plot in Fig. 3. The last three columns in Table 1 contain the differences between the orbital energies of the 3- and the 4-substituted molecules. Within the couples the molecule that reacts faster also has more stable orbitals. The position that enhances the reactivity corresponds always to the position of the substituent that better stabilizes the keto carbonyl π orbitals. This furthermore demonstrates the importance of the energy of the keto carbonyl π orbitals for the hydrogenation reactivity. It is also striking that the major contribution to the orbital difference within a couple originates from the contribution of the antibonding orbitals.

3.2. Enantioselective Hydrogenation

All diastereomeric couples given by the complexation of the trifluoroacetophenone derivatives (substrates 8–12 in Fig. 2) with cinchonidine were computed. The couples were constrained to coplanarity of substrate and anchoring group, as shown in Fig. 10 for the trifluoroacetophenone.

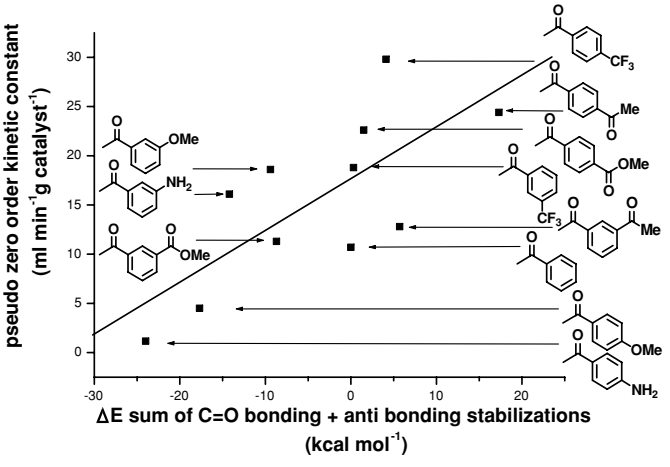

FIG. 9. Kinetic constants versus the keto carbonyl orbital energy in Van Bekkum's series (14). The energy is that of the antibonding orbital plus that of the bonding orbital with the larger coefficient.

TABLE 1

Calculated Orbital Stabilization (kcal/mol) and Pseudo-zero-order Rate Constants for a Series of Acetophenones (14)

	Kinetic constant[a]	C=O B **1**	C=O B **2**	C=O A.B.	C=O Sum	Δ B **1** 3–4[b]	Δ B **2** 3–4[c]	Δ A.B. 3–4[d]	Δ 3–4 sum
	10.7	0.0	0.0	0.0	0.0				
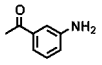	16.1	−25.7	−12.4	−1.8	−39.9	+1.6	+1.6	+8.3	+11.5
	1.16	−27.3	−14.0	−10.1	−51.4				
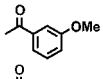	18.6	−15.8	−10.1	+0.7	−25.2	+0.6	+0.5	+7.9	+9.0
	4.5	−16.4	−10.6	−7.2	−34.2				
	18.8	+9.8	+10.1	+11.1	+31.0	−0.6	−0.1	−3.2	−3.9
	29.8	+10.4	+10.2	+14.3	+34.9				
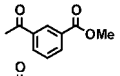	11.3	+0.1	−5.7	+11.3	+17.1	−0.2	−0.6	−10.0	−10.8
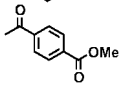	22.6	+0.3	−4.1	+21.3	+25.7				
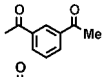	12.8	+0.1	+2.2	+10.5	+5.7	−0.1	−0.6	−8.0	−8.7
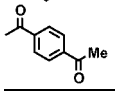	24.4	+0.2	+2.8	+18.5	+17.4				

Note. The C=O bonding (C=O B) and C=O antibonding (C=O A.B.) energies are positive when more stable and negative when less stable with respect to the corresponding orbitals of acetophenone. Bonding orbitals **1** and **2** are illustrated in Fig. 1.

[a] From (14) (ml min^{-1} g^{-1} catalyst).

[b] Energy difference of bonding C=O π orbital **1** between 3- and 4-substituted acetophenones. A positive value indicates more stable orbital for the 3-substitution.

[c] Energy difference of bonding C=O π orbital **2** between 3- and 4-substituted acetophenones. A positive value indicates more stable orbital for the 3-substitution.

[d] Energy difference of antibonding C=O π orbital between 3- and 4-substituted acetophenones. A positive value indicates more stable orbital for the 3-substitution.

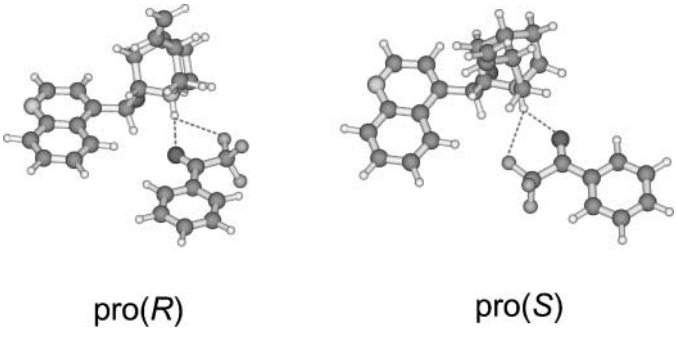

FIG. 10. Diastereomeric complexes affording the *R* and *S* products of the hydrogenation of trifluoroacetophenone.

Note that this arrangement corresponds to the proposed model for enantioselective hydrogenation (3). An orbital analysis was performed in order to find in each complex the energy level of the keto carbonyl orbitals. All compounds were hydrogenated on cinchonidine-modified platinum under standard reaction conditions (20). Table 2 lists the values of the experimental reaction rate as defined above for hydrogenation on unmodified and on modified platinum, and the e.e. values. All e.e. values correspond to enantiomeric excess of the *R*-alcohol, which was verified by comparison with the pure enantiomer. During the reaction on modified platinum a considerable part of the metal surface is occupied with the surface modifier, and therefore many catalytic sites are not accessible to the

TABLE 2

Enantioselective Hydrogenation of Some Trifluoroacetophenone Derivatives

	Rate						
	Unmodified	Modified	e.e.	ΔE A.B.[a]	ΔE B **1**[b]	ΔE B **2**[c]	ΔE sum
	3.94	4.42	(R) 36%	+1.8	+1.5	+1.9	+5.2
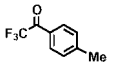	3.56	2.45	(R) 6%	+1.8	+1.3	+1.6	+4.6
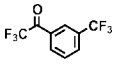	5.52	5.52	(R) 40%	+1.5	+1.8	+2.0	+5.3
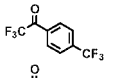	6.13	6.13	(R) 11%	+1.4	+1.3	+2.1	+4.8
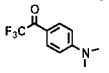	0.874	0.38	(R) 27%	+2.0	+1.6	+2.0	+5.6

Note. Experimental rates (mmol/h), enantiomeric excesses (e.e.), and calculated values (ΔE kcal/mol) for the differential stabilization of the keto carbonyl orbitals within the diastereomeric complexes are listed. Positive numbers for the differential stabilization refer to more stable orbitals in the pro(*R*) complex.

[a] Antibonding π^* orbital.

[b] Bonding π orbital **1**.

[c] Bonding π orbital **2**.

substrate (22, 23). Rates determined for the modified reaction can therefore not be directly compared to those found in the unmodified case. Nevertheless, it is interesting to note that for the unsubstituted trifluoroacetophenone, in the enantioselective hydrogenation the rate increases with respect to the racemic reaction on the unmodified catalyst. The largest differences in the rate between hydrogenation on modified and unmodified catalysts are observed for the substrates that have intrinsically low reactivity. A much weaker effect is observed in all cases where the reactivity is already high. Upon modification absolute rates remain approximately constant for the trifluoroacetophenone derivatives, with the intermediate case of the 4-dimethylamino-trifluoroacetophenone, which has the lowest reactivity within the trifluoroacetophenones, and whose rate decreases by approximately a factor two.

Table 2 also shows the differential stabilizations of the keto carbonyl orbitals in the diastereomeric complexes. Positive numbers refer to more stable orbitals in the pro(*R*) complex. Within the complexes the carbonyl π orbitals are stabilized with respect to the free molecule, which leads to an enhanced mixing of the bonding carbonyl π orbitals with the lower lying π orbitals of the aromatic ring. The resulting orbitals that are antibonding to the ring always have a higher energy than the bonding ones and are labeled in the table as **1**, while the others are labeled **2**. The criterion followed for the free molecules in the plot in Fig. 3 was to take the orbital with the largest coefficients, which was always the **2** for the trifluoroacetophenone derivatives. Within the complex the main contribution tends to come from the bonding orbital **2** in almost all cases, the only exception being the 3,5-di-trifluoromethyl acetophenone. For the differential stabilization the diagram in Fig. 11 includes contributions from both bonding orbitals (**1** and **2**), similarly to the plot in Fig. 2. The sum of all differential stabilization contributions gives invariably a positive number, which indicates a greater stabilization of the pro(*R*) complex keto carbonyl orbitals. Figure 11 clearly shows that the sum of orbital stabilizations goes in the same direction as the ΔE between the Pro(*R*) and Pro(*S*) complexes, which means that the more stable complexes have also the more stabilized keto carbonyl orbital energies.

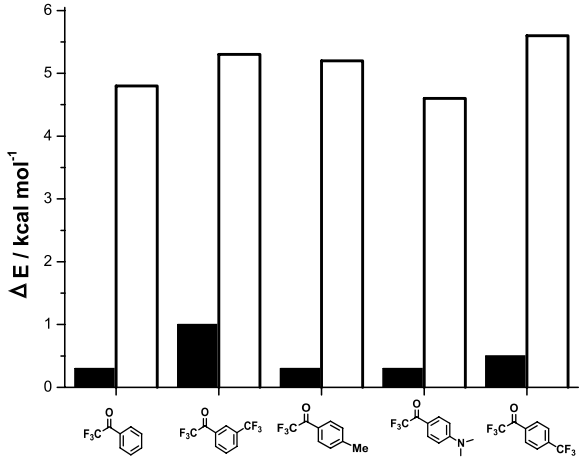

FIG. 11. Differential stability (black) and differential orbital stabilization (white) for the diastereomeric complexes formed between cinchonidine and a series of trifluoroacetophenones. Positive values indicate greater stability in the pro(*R*) complex. For the orbital energies the sum of the antibonding and bonding orbitals **1** and **2** were considered.

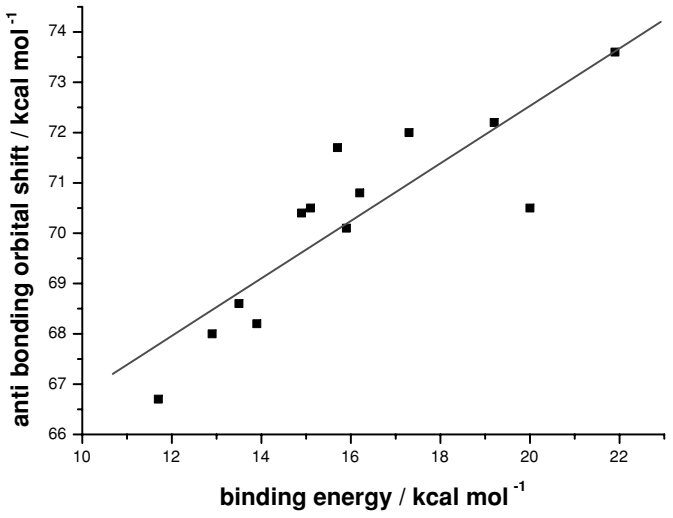

FIG. 12. Antibonding keto carbonyl orbital shift calculated as the difference between the antibonding orbital energy of the free molecule and the correspondent orbital in the pro(*R*) complex, plotted against the binding energy of the pro(*R*) complex.

Figures 12 and 13 show the behavior of the orbital stabilization as a function of the binding energy of the pro(*R*) complexes. Figure 12 shows the antibonding orbital stabilization, and Fig. 13 the sum of the three orbital stabilizations, antibonding plus bonding **1** and **2**. As reference for both, the binding energy and the orbital stabilization serve the free molecule. Despite the large deviation of some points in the plot, a clear trend is emerging: the more stable complexes have the more stabilized keto carbonyl π orbitals.

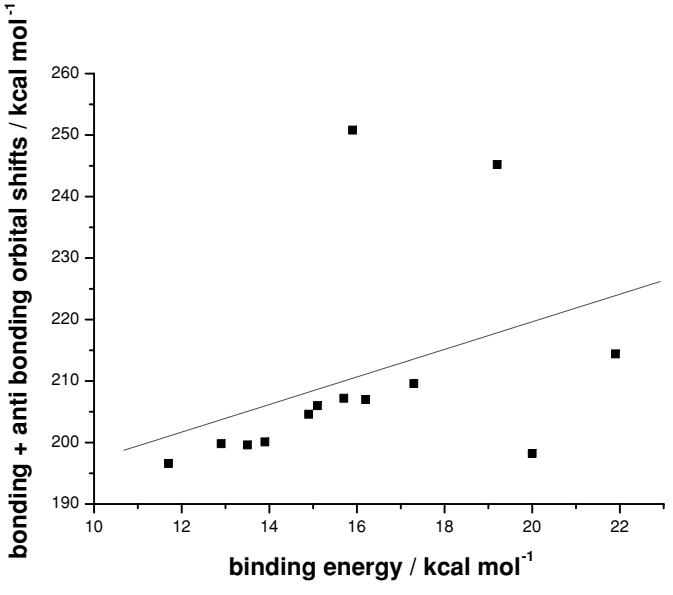

FIG. 13. Keto carbonyl orbital stabilization calculated as the sum of three contributions: the antibonding orbital and bonding orbitals **1** and **2**. The contributions are calculated as the difference between the orbital in the free molecule and the corresponding one in the pro(*R*) complex.

4. DISCUSSION

4.1. Racemic Hydrogenation

As mentioned in the introduction, the goal of the present investigation was the understanding of the kinetic aspects of the enantioselective hydrogenation of α-substituted ketones on cinchona-modified platinum and in particular also of the often observed rate acceleration. In order to understand the influence of the adsorbed chiral modifier on the reaction rate it was decided to first investigate the reactivity of the substrate on the unmodified platinum catalyst (racemic hydrogenation). The aim was to identify quantities, at the level of the electronic structure of the molecules itself, that correlate with the rates of hydrogenation. Once the intrinsic factors which affect the rate are better understood, the rate acceleration due to the surface modifier and the role of the kinetic factors for enantioselectivity should become clearer.

The results presented in the last section show that the stability of the keto carbonyl π orbitals are a good measure for reactivity, whereas carbonyl C atomic charge and the HOMO–LUMO gap are not. Hydrogenation rates should depend on the energy differences between the carbonyl orbitals and the 1s orbital of the adsorbed hydrogen since these orbitals are strongly involved in the formation of the new bond. The 1s hydrogen orbital lies lower in energy than the reactive keto carbonyl orbitals of the reactant. Therefore a stabilization of the keto carbonyl orbitals would induce an increase in orbital interaction. According to perturbation theory, at least for an early transition state, this would lead to the lowering of the energy of the transition state (Scheme 3) and consequently to an increase in the reaction rate. The good exponential correlation between rates and orbital stabilization, as shown in Figs. 2–5, and in linearized form in Fig. 6, seems to support this hypothesis. Hence it seems possible, at least for this class of substrates, to isolate one rather distinct parameter, the carbonyl orbital stabilization, affecting the reactivity toward hydrogen addition.

Scheme 2 shows a molecular orbital scheme of the mechanism of interaction. Both the bonding and the antibonding orbitals interact with the 1s orbital of activated hydrogen. Scheme 3 illustrates qualitatively the change in activation energy occurring upon orbital energy variation. The interaction between the hydrogen 1s orbital and the π system is illustrated in a Walsh diagram. The stabilization of the transition state occurs when the bonding and antibonding levels of the reactant are stabilized. As in the FMO (frontier molecular orbitals) theory (24) the energy of the transition state is extrapolated from the initial stage of the reaction to the activated complex. In this mechanistic picture

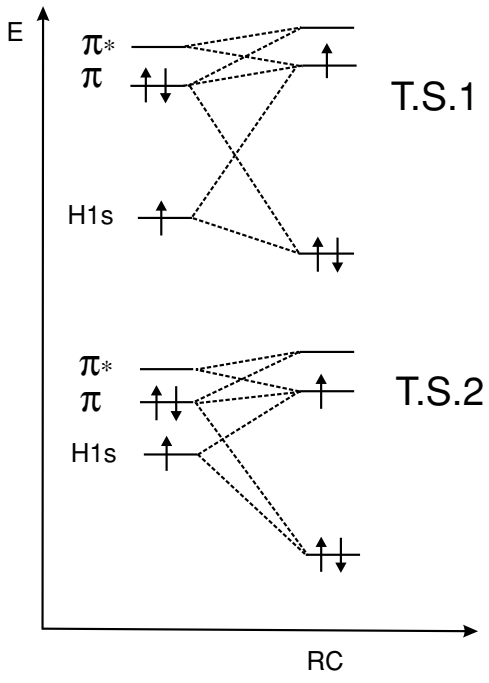

SCHEME 3. Walsh diagram for the hydrogenation reaction. On the left, the separated reactants orbital levels (adsorbed hydrogen and keto carbonyl π system of the ketone) are shown, and on the right, the orbital interactions at the transition state are shown. Bottom and top diagrams differ in the stability of the keto carbonyl π orbitals of the reactant.

activation is strictly correlated to the stabilization of the keto carbonyl orbitals.

It must be pointed out that the correlations should be searched for only where there is reason to believe that all other parameters affecting the reaction rate may be considered to have a minor influence. This can be found only within a series of compounds of similar structure.

First we focus on the correlations found for the racemic reactions. We notice that the plot in Fig. 4 shows a less clear correlation between the antibonding orbitals and the reaction rate compared to the corresponding plot for the bonding orbitals (Fig. 3). For example, 3,5-di-(trifluoromethyl) acetophenone undergoes a strong stabilization of the antibonding orbitals, but its reactivity still remains low when compared to the trifluoroacetophenones, and this is also true for the plot in Fig. 2. Note that the correlation of the antibonding orbitals also shows a separate trend between the acetophenones and the trifluoroacetophenones. The former could be very well fitted by a straight line. On the other hand the sum of the bonding and antibonding stabilizations correlates very well with the reaction rate, giving a growing exponential of a similar quality to that of Fig. 3, where only the bonding orbital stabilization are considered. The limits of taking simply the sum of the stabilizations of the π orbitals as a parameter are evident, because their contribution toward the reactivity is in general not the same.

The concept of activation of a ketone in catalytic hydrogenation on platinum through electron withdrawing groups has already been stated. Trifluoroacetophenones are believed to react faster due to the electron withdrawing effects caused by the strongly electronegative fluorine atoms. The term "electron withdrawing" should however not be taken too rigorously. Strongly electron withdrawing groups lead to a large redistribution of the electron density rather than to a net charge withdrawing (25). This is also reflected by the calculated charges (Figs. 7 and 8). Mulliken charges show that α-fluorinated acetophenones correspond to electron-rich carbonyl carbons. Confirmation comes from the results using the CHELP scheme of calculating charges. The electron enrichment of the carbonyl carbon on α-fluorination is experimentally supported by ^{13}C NMR spectroscopy, from which it can be seen that the carbonyl carbon chemical shift moves upfield and not downfield in trifluoroacetophenone with respect to acetophenone, which indicates a shielding instead of a deshielding effect of the fluorine atoms. An electron-deficient atom is not more reactive. This also emerges from a comparison between ethyl pyruvate and acetone at the level of the carbonyl carbon. The carbonyl carbon of acetone is more electron deficient (+0.52) than that of ethyl pyruvate (+0.44). Nevertheless the reactivity of ethyl pyruvate toward hydrogenation is much larger than that of acetone. Under the same reaction conditions as used for the acetophenone series, acetone has a reaction rate of 0.54 mmol/h while for ethyl pyruvate the value is 3.68 mmol/h. Also the inverse correlation, that electron-rich carbonyl carbons should react faster, does not hold in all cases. From Figs. 7 and 8 we can in fact see that compounds having a comparably electron-rich carbonyl carbon, such as the 4-dimethylamino-trifluoroacetophenone, still show a rather poor reactivity. What can on the other hand be stated is that none of the compounds studied in the acetophenone series shows a high reactivity and at the same time an electron-deficient carbonyl carbon. All fast-reacting compounds belong to the relatively electron-rich group, although as just stated, this cannot be taken as a sufficient criterion to explain the reactivity. Having mentioned the calculated charge of the carbonyl C of acetone and ethyl pyruvate, we should also add the relative energies of their keto carbonyl orbitals. The bonding keto carbonyl orbital of ethylpyruvate is 13.6 kcal/mol more stable than that of acetone, and that of its antibonding orbital is 45 kcal/mol more stable than the correspondent of acetone, which confirms the correlation observed for the acetophenone series.

The correlation found in Van Bekkum's series qualitatively confirms the result that an increasing orbital stabilization is associated with an increasing reactivity. Note that these reactions were performed on a palladium catalyst, whereas ours were platinum catalyzed. This suggests that our observations may not be restricted to one particular

metal and may represent an intrinsic reactivity of the ketone toward hydrogen addition.

Within the couples of 3- and 4-substituted acetophenones the major contribution on the orbital differentiation is given by the antibonding π orbital. This last observation confirms that the contribution of the antibonding orbital to the reactivity may be critical, although not equally important in all cases. While the importance of the keto carbonyl π orbital stabilization seems to be confirmed by all analyses, the different roles played by the bonding and the antibonding orbitals is less clear. Differences in the relative importance of bonding and antibonding π orbitals for the reactivity may arise due to the kind of compound, the metal, and the position of the substituent. Therefore, still, sums of orbital stabilization are, although not always the best, the most general parameters.

4.2. Enantioselective Hydrogenation

The concept just outlined is able to explain also another well-known phenomenon observed in this class of reaction, that is, the rate acceleration in the presence of a chiral surface modifier. This phenomenon is well-known for this class of reactions, in particular for the hydrogenation of ethyl pyruvate in the presence of cinchonidine, which was often used as a model reaction. Although the number of accessible active platinum sites on the catalyst decreases due to the adsorbed modifier, whose presence on the surface has been recently confirmed through vibrational spectroscopy (22, 23), the reaction is accelerated by the same modifier. The model of interaction between reactant and modifier used to rationalize enantiodifferentiation implies the presence of a hydrogen bond between the quinuclidine nitrogen atom and the carbonyl group of the substrate, as shown in Fig. 10. This interaction leads to a net stabilization of the keto carbonyl orbitals of the substrate. The amount of this stabilization changed according to the strength of the interaction but always comprised between 50 and 100 kcal/mol per orbital. Table 2 contains the sums of the differential stabilizations calculated for the diastereomeric complexes formed between the trifluoroacetophenone derivatives and cinchonidine (ΔE (pro(R)-(pro(S)) and shows that the pro(R) complexes have more-stable keto carbonyl orbitals than the pro(S). Based on the elaborated correlation between reactivity and stability of the keto carbonyl π orbitals this would lead to a larger hydrogenation rate for the pro(R) complexes. On the other hand we have seen (Fig. 11) that all the pro(R) are also more stable than the pro(S) complexes. Therefore, in our model, both elements direct the reaction toward the formation of the R enantiomer selectively. On the one hand thermodynamics favors the formation of the pro(R) complex. On the other hand the larger stability of the carbonyl π orbitals promotes hydrogenation of the pro(R) with respect to the pro(S) complex. It therefore seems that for the reactions of the trifluoroacetophenone derivatives investigated here, Scheme 1c is most likely. The correlation between the stability of the complex and the consequent stability of the orbitals is not very rigid and reveals a trend more than a quantitative correlation. This is mainly a consequence of the fact that the orbital energy is critically dependent on the energy of the hydrogen bond (Fig 13), which in turn depends on the geometry of interaction. New interaction geometries are now being studied in order to take into account also the possible formation of a second hydrogen bond interaction between the hydroxylic functional group of cinchonidine and the ketone. Nevertheless, irrespective of the interaction geometry, the hydrogen bond always leads to keto carbonyl orbital stabilization, and diastereomeric complexes, having different energies, are bound to have differentially stabilized orbitals. The conclusions reached for one particular interaction mode in the present discussion can be safely extended to other cinchonidine–reactant complexes bearing different constraints and different binding modes.

5. CONCLUSIONS

The electronic structure analysis of a series of acetophenone derivatives has shown that the energy levels of the orbitals which are involved in hydrogenation can be correlated with the reactivity of the compounds. This insight is consistent with the rate acceleration of the catalytic hydrogenation of substituted ketones that is often observed on platinum–cinchona systems, because the modifier–reactant interaction stabilizes the keto carbonyl orbitals. Within the one-to-one interaction model this approach also shows that the more stabilized diastereomeric complexes also undergo a larger stabilization of the keto carbonyl orbitals, leading to the important observation that both thermodynamic and kinetic effects direct the reactivity toward the formation of the same enantiomer, as exemplified in Scheme 1c. This explains the success of the previous model based on thermodynamic considerations alone, in predicting the direction of enantioselectivity. These same concepts are also easily extendable to interaction modes between the modifier and the reactant that are different from that in Fig. 10.

ACKNOWLEDGMENTS

Computing time has been provided by the ETH Zurich and by the Swiss center for Scientific Computing (CSCS) in Manno. Financial support of the Swiss National Foundation is kindly acknowledged.

REFERENCES

1. Baiker, A., and Blaser, H. U., *in* "Handbook of Heterogeneous Catalysis" (G. Ertl, H. Knözinger, and J. Weitkamp, Eds.), Vol. 5, p. 2422, VCH, Weinheim, 1997.
2. Blaser, H. U., Jalett, H. P., Müller, M., and Studer, M., *Catal. Today* **37**, 441 (1997).
3. Baiker, A., *J. Mol. Catal. A* **115**, 473 (1997).

4. Wells, P. B., and Wilkinson, A. G., *Topics Catal.* **5**, 39 (1998).
5. Baiker, A., *Curr. Opin. Solid State Mater. Sci.* **3**(1), 86 (1998).
6. Baiker, A., *J. Mol. Catal. A* **163**, 205 (2000).
7. Schwalm, O., Weber, J., Margitfalvi, J., and Baiker, A., *J. Mol. Struct.* **297**, 285 (1993); Schwalm, O., Minder, B., Weber, J., and Baiker, A., *Catal. Lett.* **23**, 271 (1994); Schwalm, O., Weber, J., Minder, B., and Baiker, A., *Int. J. Quantum Chem.* **52**, 191 (1994); Schwalm, O., Weber, J., Minder, B., and Baiker, A., *J. Mol. Struct.* **330**, 353 (1995).
8. Simons, K. E., Meheux, P. A., Griffiths, S. P., Sutherland, I. M., Johnston, P., Wells, P. B., Carley, A. F., Rajumon, M. K., Roberts, M. W., and Ibbotson, A., *Recl. Trav. Chim. Pays-Bas* **113**, 465 (1994).
9. Bürgi, T., and Baiker, A., *J. Catal.* **194**, 445 (2000).
10. Schürch, M., Schwalm, O., Mallat, T., Weber, J., and Baiker, A., *J. Catal.* **169**, 275 (1997).
11. Vargas, A., Bürgi, T., and Baiker, A., *J. Catal.* **197**, 378 (2001).
12. Baiker, A., *in* "Chiral Catalyst Immobilization and Recycling" (D. E. de Vos, I. F. J. Vankelecom, and P. A. Jacobs, Eds.), p. 155. Wiley–VCH, Weinheim/New York, 2000.
13. Landis, C. R., and Halpern, J., *J. Am. Chem. Soc.* **109**, 1746 (1987).
14. Van Bekkum, H., Kieboom, A. P. G., and Van de Putte, K. J. G., *Recl. Trav. Chim. Pays-Bas* **88**, 53 (1969).
15. Frisch, M. J., Trucks, G. W., Schlegel, H. B., Scuseria, G. E., Robb, M. A., Cheeseman, J. R., Zakrzewski, V. G., Montgomery, J. A., Stratmann, R. E., Burant, J. C., Dapprich, S., Millam, J. M., Daniels, A. D., Kudin, K. L., Strain, M. C., Farkas, O., Tomasi, J., Barone, V., Cossi, M., Cammi, R., Mennucci, B., Pomelli, C., Adamo, C., Clifford, S., Ochterski, J., Johnson, B. G., Petersson, G. A., Ayala, P. Y., Cui, Q., Morukuma, K., Malik, D. K., Rabuk, A. D., Raghavachari, K., Foresman, J. B., Cioslowski, J., Ortiz, J. V., Stefanov, B. B., Liu, G., Liashenko, A., Piskorz. P., Kamaromi, I., Gomperts, R., Martin, R. L., Fox, D. J., Keith, T., Al-Laham, M. A., Peng, C. Y., Nanayakkara, A., Gonzalez, C., Challacombe, M., Gill, P. M. W., Johnson, B. J., Chen, W., Wong, M. W., Andres, J. L., Head-Gordon, M., Replogle, E. S., and Pople, J. A., Gaussian 98, Revision A.1. Gaussian, Pittsburgh, 1998.
16. Mulliken, R. S., *J. Chem. Phys.* **23**, 1833 (1955).
17. Chirlian, L. E., and Francl, M. M., *J. Comp. Chem.* **8**, 894 (1987).
18. Schaftenaar, G., and Noordik, J. H., *J. Comput.-Aided Mol. Design* **14**, 123 (2000).
19. von Arx, M., Mallat, T., and Baiker, A., *J. Catal.* **193**, 161 (2000).
20. von Arx, M., Mallat, T., and Baiker, A., *Tetrahedron Asymmetry* **12**, 3089 (2001).
21. Hammett, L. P., "Physical Organic Chemistry." McGraw-Hill, New York, 1970.
22. Ferri, D., Bürgi, T., and Baiker, A., *Chem. Commun.* 1172 (2001).
23. Ferri, D., and Bürgi, T., *J. Am. Chem. Soc.* **123**, 12074 (2001).
24. Fleming, I., "Frontier Orbitals and Organic Chemical Reactions." Wiley, New York, 1976.
25. March, J., "Advanced Organic Chemistry." Wiley, New York, 1992.